Short Article

Cell Stem Cell

Functional Correction of Large Factor VIII Gene Chromosomal Inversions in Hemophilia A Patient-Derived iPSCs Using CRISPR-Cas9

Graphical Abstract

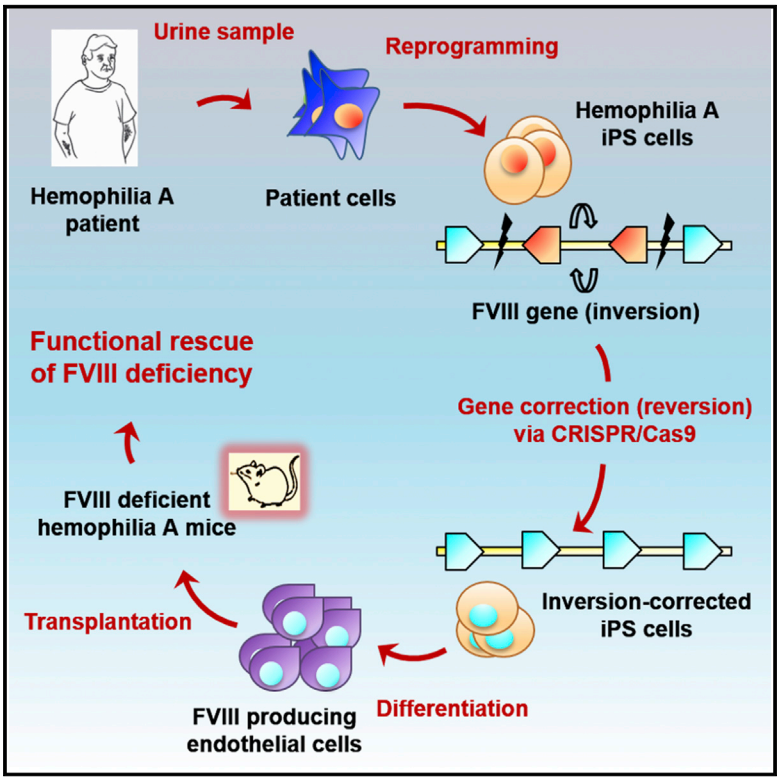

Highlights

- CRISPR-Cas9 and targeted sgRNAs can revert large inversions in hemophilia A iPSCs
- Endothelial cells derived from corrected iPSCs express correctly spliced Factor VIII
- Transplantation of corrected iPSCs can rescue injury mortality in hemophiliac mice
- Whole-genome and targeted deep sequencing did not detect off-target mutations

Authors

Chul-Yong Park, Duk Hyoung Kim, Jeong Sang Son, ..., Jong-Hoon Kim, Dong-Wook Kim, Jin-Soo Kim

Correspondence

dwkim2@yuhs.ac (D.-W.K.), jskim01@snu.ac.kr (J.-S.K.)

In Brief

Park et al. used CRISPR-Cas9 in patient iPSCs to correct two large inversions that are the most common underlying mutations for severe hemophilia, and they show that the correction is functional by rescuing lethality in hemophiliac mice using iPSC-derived endothelial cells.

Park et al., 2015, Cell Stem Cell *17*, 213–220
August 6, 2015
http://dx.doi.org/10.1016/j.stem.2015.07.001

CellPress

Cell Stem Cell
Short Article

Functional Correction of Large Factor VIII Gene Chromosomal Inversions in Hemophilia A Patient-Derived iPSCs Using CRISPR-Cas9

Chul-Yong Park,[1,6] Duk Hyoung Kim,[2,3,6] Jeong Sang Son,[4,6] Jin Jea Sung,[1] Jaehun Lee,[4] Sangsu Bae,[5] Jong-Hoon Kim,[4,7] Dong-Wook Kim,[1,7,*] and Jin-Soo Kim[2,3,7,*]
[1]Department of Physiology and Brain Korea 21 Plus Project for Medical Science, Yonsei University College of Medicine, Seoul 120-752, Korea
[2]Center for Genome Engineering, Institute for Basic Science, Seoul 151-742, Korea
[3]Department of Chemistry, Seoul National University, Seoul 151-742, Korea
[4]Laboratory of Stem Cell Biology, Division of Biotechnology, College of Life Science and Biotechnology, Korea University, Seoul 136-713, Korea
[5]Department of Chemistry, Hanyang University, Seoul 133-791, Korea
[6]Co-first author
[7]Co-senior author
*Correspondence: dwkim2@yuhs.ac (D.-W.K.), jskim01@snu.ac.kr (J.-S.K.)
http://dx.doi.org/10.1016/j.stem.2015.07.001

SUMMARY

Hemophilia A is an X-linked genetic disorder caused by mutations in the *F8* gene, which encodes the blood coagulation factor VIII. Almost half of all severe hemophilia A cases result from two gross (140-kbp or 600-kbp) chromosomal inversions that involve introns 1 and 22 of the *F8* gene, respectively. We derived induced pluripotent stem cells (iPSCs) from patients with these inversion genotypes and used CRISPR-Cas9 nucleases to revert these chromosomal segments back to the WT situation. We isolated inversion-corrected iPSCs with frequencies of up to 6.7% without detectable off-target mutations based on whole-genome sequencing or targeted deep sequencing. Endothelial cells differentiated from corrected iPSCs expressed the *F8* gene and functionally rescued factor VIII deficiency in an otherwise lethal mouse model of hemophilia. Our results therefore provide a proof of principle for functional correction of large chromosomal rearrangements in patient-derived iPSCs and suggest potential therapeutic applications.

INTRODUCTION

Hemophilia A is one of the most common genetic disorders, with an incidence of 1 in 5,000 male births in the US; it is caused by various mutations in the blood coagulation factor VIII (*F8*) gene on chromosome X. Depending on mutant genotypes, clinical symptoms range from mild (5%–30% F8 activity, 50% of all hemophilia A patients) to moderate (2%–5% activity, 10%) to severe (<1% activity, 40%) (Graw et al., 2005). Nearly half of all severe hemophilia A patients harbor one of the two different types of gross chromosomal inversions, rather than point mutations, that involve the *F8* intron 1 homolog (int1h) (a minor type, ~5% of severe hemophilia A cases) or the intron 22 homolog (int22h) (a major type, ~40%). These two large inversions result from erroneous repair of DNA double-strand breaks (DSBs) accidently induced in the homologs via non-allelic homologous recombination (NAHR).

Previously, we had used custom-made zinc-finger nucleases (ZFNs) in immortalized WT human cell lines (Lee et al., 2012) and transcriptional activator-like effect nucleases (TALENs) in WT induced pluripotent stem cells (iPSCs) (Park et al., 2014) to invert the chromosomal segment between the two identical int1h sequences (designated hereinafter int1h-1 and int1h-2), which are separated by 140 kilobase pairs (kbp), at a frequency of 0.1% and 1.9%, respectively. This process mimicked the erroneous DSB repair, artificially inducing the inversion genotype.

The other 600-kbp inversion involving three int22h sequences (designated int22h-1, -2, and -3) is eight times more prevalent than is the 140-kbp inversion, but it is technically more challenging to revert partially due to the larger size of the inverted region and the presence of three, rather than two, homologs on chromosome X. Furthermore, because int22h is much larger (10 kbp) than int1h (1 kbp), it is very difficult to genotype the int22h inversion or its reversion using conventional PCR: the entire 10-kbp int22h must be amplified. In fact, to the best of our knowledge, it has never been shown that the 600-kbp chromosomal segment involving int22h can be reverted in human cells, not to mention in patient-derived iPSCs, using programmable nucleases. In this study, we used the type II clustered, regularly interspaced short palindromic repeat (CRISPR)/CRISPR-associated (Cas) system, a.k.a. RNA-guided engineered nucleases (RGENs) (Cho et al., 2013; Mali et al., 2013; Cong et al., 2013; Cho et al., 2014), to revert these two large inverted regions back to the normal orientation in hemophilia A patient-derived iPSCs. We also showed that endothelial cells differentiated from the inversion-corrected iPSCs expressed the *F8* gene in vitro and rescued the F8 deficiency in a hemophilia mouse model, demonstrating a proof of principle for cell-based hemophilia therapy.

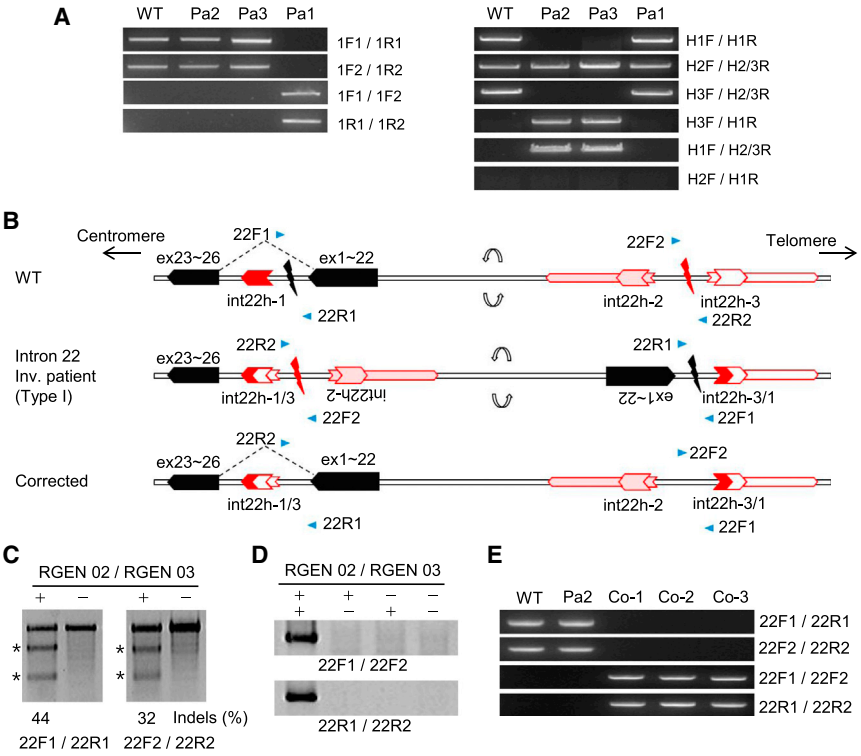

Figure 1. Correction of the Partially Inverted *F8* Gene in Hemophilia A Patient-Derived iPSCs

(A) Genomic DNA was isolated from human dermal fibroblasts (WT) and hemophilia A patient-derived urine cells (Pa1, Pa2, and Pa3) and subjected to PCR analysis using appropriate primers shown in Figure S1A and a previous report (Bagnall et al., 2006) to detect the intron 1 (left) or 22 (right) inversions.

(B) Schematic representation of intron 22 inversion and reversion. Three homolog regions are shown as int22h-1, int22h-2, and int22h-3. Blue arrowheads indicate PCR primers. Nuclease target sites near int22h-1 or int22h-3 are shown as black (RGEN 02) or red (RGEN 03) lightning symbols.

(C) Mutations at nuclease target sites in HeLa cells were confirmed by the T7E1 assay.

(D) PCR products corresponding to the inversion of the 563-kbp chromosomal segment in HeLa cells.

(E) PCR analysis to confirm inversion correction in iPSC clones.

(F) DNA sequences of breakpoint junctions in the inversion-corrected iPSC clones. Each RGEN target sequence is underlined. The PAM sequence is shown in green. Dashes indicate deleted bases. Lowercase letters indicate inserted bases. Two blue arrows indicate cleavage sites.

See also Figures S1 and S2 and Table S1.

RESULTS

First, we genotyped 11 unrelated, severe hemophilia A patients and identified one patient with the int1 inversion and three patients with the int22 inversion. We chose the one patient with the int1 inversion (termed Pa1) and two patients with the int22 inversion (termed Pa2 and Pa3) for further study (Figure 1A). We established their respective iPSCs by introducing the four Yamanaka factors via an episomal vector or Sendai virus into urinary epithelial cells, avoiding an invasive biopsy to obtain fibroblasts from these patients with this bleeding disorder.

In parallel, we tested RGENs, which consisted of the Cas9 protein and a small guide RNA (sgRNA), for their ability to induce or revert these two inversions in WT HeLa cells and patient iPSCs. RGEN 01 was designed to target a site in int1h (Figure S1A). This RGEN can cleave two identical sites, one in int1h-1 and the other in its homolog, int1h-2, that is located 140 kbp upstream. Inversions can occur via NAHR or non-homologous end joining (NHEJ). RGEN 01 was highly active, inducing small insertions and deletions (indels) at a frequency of 34% at the target site in int1h (Figure S1B). In addition, RGEN 01 induced the inversion of the 140-kbp chromosomal segment in HeLa cells, as shown by inversion-specific PCR (Figure S1C). The frequency of this inversion ranged from 2.2% to 3.1%, as measured by digital PCR (Table S1) (Kim et al., 2010; Lee et al., 2010). We determined the DNA sequences of the inversion-specific PCR amplicons and found that indels were induced at the two inversion breakpoint junctions (Figure S1D). Encouraged by this high frequency, we co-transfected plasmids encoding the Cas9 protein and the sgRNA into iPSCs derived from Pa1 (Pa1-iPSCs) and analyzed iPSC colonies using PCR. Eight colonies (not necessarily derived from single cells) out of 120 colonies (6.7%) produced positive PCR bands on an agarose gel. Four colonies were then further cultured to obtain single-cell-derived clones. These clones produced PCR amplicons corresponding to the int1h-1 and int1h-2 regions, indicating that the inverted 140-kbp chromosomal segment in Pa1 cells was reverted (Figure S1E). In contrast, no such PCR amplicons were produced from Pa1 iPSCs or urinary cells. We sequenced the PCR amplicons and found that no indels were induced at the target site in three clones. In the other clone, there was a 13-bp deletion at the target site (Figure S1F).

We then focused on the other larger and more prevalent int22h inversion. To rule out the possibility that unwanted deletions or inversions involving any two of the three int22 homologs, rather than the desired reversion of the inverted 600-kbp segment, were induced by cutting a site within int22h, we used two RGENs that target sites outside of the homologs (Figure 1B). This strategy also facilitated detection of the reversion event using

appropriate PCR primers: amplification of two ~1-kbp segments outside of int22h rather than chromosomal segments that spanned the entire 10-kbp int22h allowed genotyping.

We designed two RGENs (termed RGEN 02 and RGEN 03) to target sites near int22h-1 and int22h-3 and tested their nuclease activity in HeLa cells using the T7 endonuclease I (T7E1) assay. These RGENs were highly active, inducing indels at each target site with a frequency of 44% or 32% (Figure 1C). Next, we used PCR to detect the inversion of the 563-kbp chromosomal segment between the two target sites. Transfection of either RGEN 02 or RGEN 03 alone into HeLa cells did not produce inversion-specific PCR amplicons. In contrast, co-transfection of these RGEN plasmids gave rise to two inversion-specific PCR amplicons (Figure 1D). The inversion frequency was in the range of 1.5% to 2.2% (Table S1). We determined the DNA sequences of the PCR amplicons and found that indels accompanied most of the two inversion breakpoint junctions, supporting the idea that two DSBs induced by the two RGENs were repaired by error-prone NHEJ (Figure S2A). Note that HeLa cells are WT with respect to the *F8* exon orientation. In Pa2 and Pa3 cells, *F8* exons 1 to 22 are inverted. But still, the two RGEN target sites are conserved, enabling the reversion of the large chromosomal segment.

Next, we transfected RGEN 02 and 03 into Pa2 iPSCs using an electroporator, and we isolated 135 colonies whose genomic DNA samples were subjected to PCR analysis. Five colonies (3.7%) yielded PCR amplicons corresponding to the inversion-correction (namely reversion) event. No such PCR products were obtained using genomic DNA isolated from Pa2 iPSCs or WT iPSCs (Figure 1E). These colonies were further expanded to enable isolation of three independent single-cell-derived clones. We then determined the DNA sequences at the two inversion breakpoint junctions, which confirmed the reversion of the 563-kbp chromosomal segment between the two RGEN sites (Figure 1F). As in HeLa cells, indels, characteristic of error-prone NHEJ, were observed at the two breakpoint junctions in these inversion-corrected iPSCs.

We then investigated whether the inversion-corrected iPSCs remained pluripotent. First, we checked the expression of stem cell marker genes in inversion-corrected Pa1 (int1h inversion) and Pa2 (int22h inversion) iPSCs and found that four marker genes, namely, *OCT4*, *SOX2*, *LIN28*, and *NANOG*, were transcribed actively in these cells (Figure 2A). Second, these inversion-corrected iPSCs were successfully differentiated into three primary germ layers (Figure 2B). Furthermore, they showed a normal karyotype (Figure 2C). Taken together, these results show that gross chromosomal reversions induced by RGENs do not negatively affect the pluripotency of patient-derived iPSCs.

Endothelial cells derived from mesoderm are a major source of *F8* gene expression (Shahani et al., 2010). We differentiated patient iPSCs and inversion-corrected patient iPSCs into mesoderm and measured the levels of *F8* mRNA using RT-PCR. As expected, no PCR bands corresponding to *F8* exons 1 and 2 were detected in cells differentiated from Pa1-iPSCs, indicating that *F8* was not expressed in patient-derived cells (Figure 2D). In contrast, PCR bands corresponding to these exons were detected in cells differentiated from the WT iPSCs or the two inversion-corrected Pa1-iPSCs (termed Co-1 and Co-2). Likewise, PCR amplicons corresponding to *F8* exons 22 and 23 were not detected in cells differentiated from Pa2- and Pa3-iPSCs, but were detected in cells differentiated from the three inversion-corrected iPSCs (Figure 2D). We also performed Sanger sequencing to confirm that exons 1 and 2 or exons 22 and 23 were spliced correctly in cells differentiated from the inversion-corrected iPSCs (Figure 2E). These results prove that the *F8* gene was repaired in patient iPSCs that had harbored intron 1 and 22 inversions, supporting the expression of the *F8* gene in mesoderm cells.

Next, we further differentiated WT, patient-derived, and inversion-corrected iPSCs into mature endothelial cells (Merkely et al., 2015) and checked the expression of the F8 protein by immunocytochemistry. As expected, the endothelial cells differentiated from the WT and the three inversion-corrected Pa1-iPSC clones (termed Pa1 Co-1 to Pa1 Co-3) expressed the F8 protein (Figures 3A and S3). In contrast, no signals corresponding to the F8 protein were detected in cells differentiated from Pa1-iPSCs, although these cells differentiated into mature endothelial cells, as shown by the expression of von Willebrand factor, a marker protein of mature endothelial cells (Figure 3A). Because the entire amino acid sequence of the F8 protein is still expressed as two inactive polypeptide chains in cells with the int22h inversion (Pandey et al., 2013), positive signals were detected in mature endothelial cells derived from both Pa2 iPSCs (int22h inversion) and inversion-corrected Pa2 iPSCs (termed Pa2 Co-1 to Pa2 Co-3). This implies that no neutralizing antibodies against the F8 protein will be produced in patients transplanted with the int22h inversion-corrected cells.

To test whether endothelial cells differentiated from inversion-corrected iPSCs could functionally rescue the F8 deficiency in an animal model, we transplanted endothelial cells generated from patient iPSCs (Pa2) and inversion-corrected iPSCs (Pa2 Co-1) into the hind-limb of hemophilia A mice whose *F8* gene was disrupted. Two weeks after transplantation, these mice were subjected to a tail-clip challenge. All hemophilia mice (n = 5) that had not received a transplant, as well as those (n = 9) transplanted with Pa2-derived cells, soon died; the average survival time was 71 min and 65 min, respectively (Figure 3B). Notably, three out of nine mice transplanted with cells derived from the Pa2 Co-1 iPSCs were alive 2 days after the tail-clip challenge, which was the end point of this experiment. Furthermore, the other six mice that did not survive the challenge also showed a significant increase in the survival time (111 min on average) compared to non-transplanted mice or mice transplanted with Pa2-derived cells (Figure 3C). We then measured the F8 enzymatic activity in plasma samples obtained from these hemophilia mice and WT mice using a chromogenic assay. The relative F8 activity in mice transplanted with Pa2 Co-1 iPSC-derived cells was 10% of that in WT mice, significantly higher than that in non-transplanted mice (3.3%) and those transplanted with Pa2 iPSC-derived cells (4.3%) (Figure 3D). Taken together, these results indicate that the F8 deficiency in hemophilia mice can be functionally rescued by transplantation of endothelial cells derived from inversion-corrected iPSCs.

To prevent unwanted insertions of plasmid fragments at RGEN on-target and off-target sites, we transfected recombinant Cas9 protein purified after expression in *E. coli* and in vitro transcribed sgRNAs (termed RGEN ribonucleoproteins, or RNPs), rather

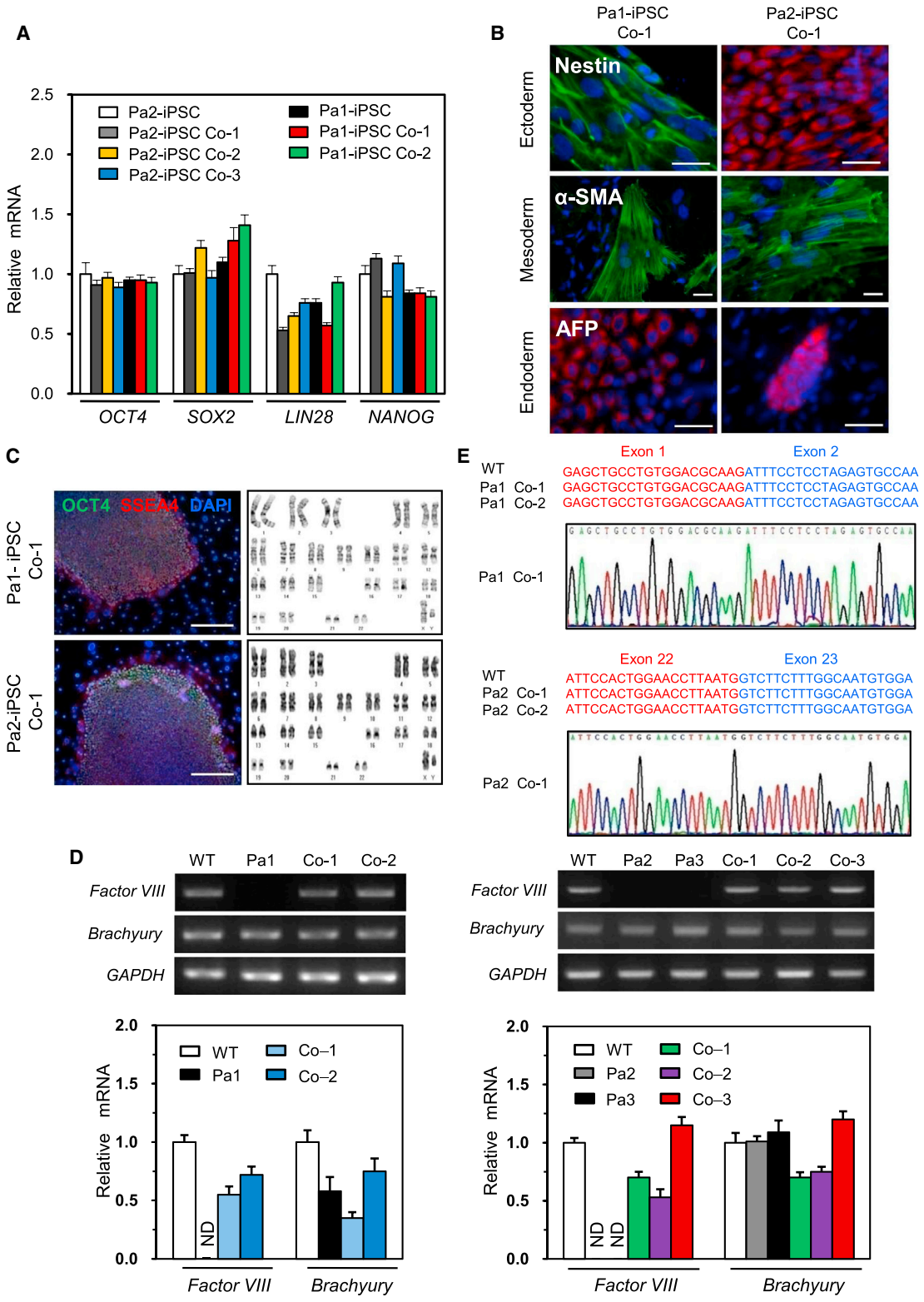

Figure 2. Characterization of Inversion-Corrected iPSC Clones

(A) Quantitative real-time PCR (qPCR) was carried out to detect endogenous *OCT4*, *SOX2*, *LIN28,* and *NANOG* mRNAs from parental and corrected cell lines. The expression level of each gene was normalized to that of *GAPDH*.

(B) In vitro differentiation of inversion-corrected lines. The expression of marker proteins representing ectoderm (Nestin), mesoderm (α-smooth muscle actin [α-SMA]), and endoderm (α-fetoprotein [AFP]) in corrected lines is shown. Scale bar, 50 μm.

(legend continued on next page)

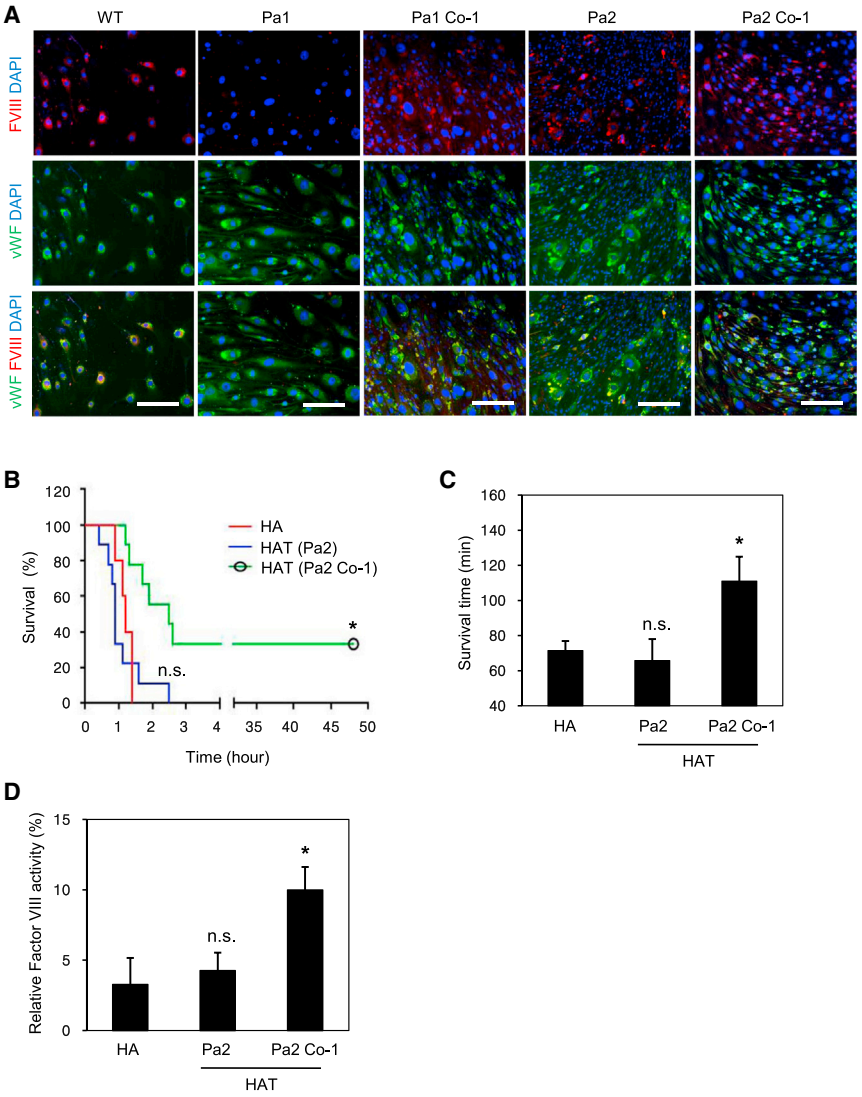

Figure 3. Functional Rescue of the Factor VIII Deficiency in Hemophilia Mice Using Inversion-Corrected iPSCs

(A) The F8 protein in endothelial cells differentiated from WT, patient iPSCs (Pa1 and Pa2), and inversion-corrected iPSCs (Pa1 Co-1 and Pa2 Co-1) was detected by immunocytochemistry. DAPI signals (blue) indicate the total cell presence in the image. FVIII, F8 protein; vWF, von Willebrand factor (a marker protein for mature endothelial cells). Scale bar, 100 μm.

(B) Proportions of surviving mice after the tail-clip challenge. HA, hemophilia mice (n = 5); HAT, hemophilia mice transplanted with cells derived from Pa2 iPSCs (n = 9) or Pa2 Co-1 iPSCs (n = 9). n.s., not significant compared with HA; *p < 0.01 compared with the Pa2 group (log-rank test).

(C) Average survival time of mice that died after the tail-clip challenge. Note that the three out of nine hemophilia mice transplanted with Pa2 Co-1 cells that survived the challenge were excluded in this analysis. n.s., not significant compared with HA; *p < 0.05 compared with the Pa2 group (Student's t test).

(D) Relative factor VIII activities were determined in plasma obtained from non-transplanted hemophilia A mice (HA, n = 5) or transplanted hemophilia A mice (HAT, n = 9 each). Data are presented as the percent of the F8 activity in WT mice (100%, n = 4). n.s., not significant compared with HA; *p < 0.05 compared with the Pa2 group (Student's t test).

See also Figure S3.

than plasmids encoding these components, into two patient (Pa1 and Pa3) iPSCs, each harboring an intron 1 or 22 inversion. We used PCR and Sanger sequencing to confirm the reversion of the 140-kbp or 563-kbp chromosomal segments in these iPSCs, restoring the genetic integrity of the *F8* gene (Figures S2B and S2C). RGEN RNP delivery can also reduce off-target effects without sacrificing genome editing activity at on-target sites, because RNPs, unlike plasmids, cleave chromosomal target DNA immediately after transfection and are rapidly degraded in cells (Kim et al., 2014).

RGENs can induce off-target mutations at sites homologous in sequence with on-target sites (Cho et al., 2014; Cradick et al., 2013; Fu et al., 2013; Hsu et al., 2013; Pattanayak et al., 2013). We investigated whether the RGENs used in this study left any collateral damage in addition to inversion corrections in patient iPSCs using targeted deep sequencing and whole-genome sequencing (WGS). First, we searched for potential off-target sites that differed from the three RGEN on-target sites by up to four nucleotides in the human genome using Cas-OFFinder, a web-based program accessible at http://www.rgenome.net (Bae et al., 2014). A total of 31, 44, and 43 potential off-target sites for RGEN 01, RGEN 02, and RGEN 03, respectively, were tested in a total of six inversion-corrected iPSC clones (three int1h clones and three int22h clones) using targeted deep sequencing. No off-target indels were found at these sites (Table S2).

Next, genomic DNA isolated from original patient (Pa1 and Pa2) iPSCs and respective inversion-corrected iPSCs (Pa1 Co-1 and Pa2 Co-1) were subjected to WGS. We focused on indels rather than substitutions because programmable nucleases

(C) The expression of OCT4 and SSEA4, human-ESC-specific markers, was detected by immunocytochemistry. Scale bar, 100 μm. Karyotypes of the indicated iPSC lines are shown.

(D) *F8* gene expression in cells differentiated from intron 1 and 22 inversion-corrected iPSC lines. RT-PCR (upper) and qPCR (lower) was used to detect expression of *F8* and a mesoderm marker gene (*Brachyury*) in cells derived from WT iPSCs, patient iPSCs (Pa1, Pa2 and Pa3), and inversion-corrected Pa1- (Co-1 and Co-2) or Pa2-iPSCs (Co-1, Co-2 and Co-3). *GAPDH* expression was used as a loading control. ND, not detected.

(E) Chromatograms showing correct splicing between exons 1 and 2 or exons 22 and 23 in inversion-corrected iPSC lines (related to Figure 2D).

See also Figure S3, Table S2, and Table S3.

including RGENs rarely produce point mutations (Kim et al., 2013; Bae et al., 2014). First, we used Isaac, a variant calling program, to identify indels relative to the hg19 reference genome. We applied bioinformatics filters to discard indels that were listed in a public database, those that were also called in respective patient genomes that harbored the int1h or int22h inversion and the other inversion-corrected genome, and those that occurred at homo-polymer or repeat sequences due to sequencing errors. As a result, 9,848 to 13,707 indels that were unique in each inversion-corrected genome sequence were obtained. Next, we compared RGEN target sites with WT loci corresponding to the indel locations. Only 31 to 106 indel sites contained a 5′-N(G/A)G-3′ PAM sequence and had at least 12 nucleotide matches with respective on-target sequences (Table S3). We then determined the DNA sequences corresponding to these indels in the two inversion-corrected genomes. None of the indels were validated by targeted deep sequencing. Second, we computationally identified all the potential off-target sites that differed from on-target sites by up to eight nucleotides or that differed by up to two nucleotides with a DNA or RNA bulge of up to five nucleotides in length in the sequence genomes using Cas-OFFinder. We then compared sequence reads aligned around each of the resulting 511,700 to 937,778 candidate off-target sites with the reference sequence (Table S3). No off-target indels were identified. These results show that the three RGENs used in this study did not leave off-target mutations in the inversion-corrected patient iPSCs, in line with a recent report demonstrating high specificity of RGENs in clonal populations of pluripotent stem cells (Veres et al., 2014).

DISCUSSION

Genome-wide off-target effects are of particular concern for RGEN applications in gene and cell therapy (Koo et al., 2015). Recently, we and several other groups have independently presented various methods for profiling genome-wide RGEN off-target sites in a bulk population of cells (Kim et al., 2015; Wang et al., 2015; Tsai et al., 2015; Frock et al., 2015; Ran et al., 2015). Although RGENs show a broad spectrum of specificities, mutation frequencies at off-target sites that differ from on-target sites by three or more nucleotides are at least a few orders of magnitude lower than those at respective on-target sites. This means that the probability of finding off-target mutations in a clonal population of cells is very low if one chooses a unique target site in the human genome. In fact, WGS or whole-exome sequencing analyses showed that nuclease-induced off-target mutations were not present in individual clones of gene knockout cells (Veres et al., 2014; Smith et al., 2014; Suzuki et al., 2014; Cho et al., 2014; Kim et al., 2015).

In this study, we chose unique target sequences that differ from any other site in the human genome by at least three nucleotides to avoid off-target effects. Furthermore, we used guide RNAs with two extra, unmatched guanine nucleotides at the 5′ terminus, which reduce off-target effects by orders of magnitude without sacrificing mutation efficiencies at on-target sites. Genome-wide off-target sites can still be identified in a bulk population of cells in an unbiased manner using Digenome-seq and other methods. However, in this study, we isolated single-cell derived clones. In line with previous studies, targeted deep sequencing and WGS analyses showed that no off-target mutations were induced by these RGENs in inversion-corrected iPSCs.

In summary, we used RGENs to repair two recurrent, large chromosomal inversions responsible for almost half of all severe hemophilia A cases in patient-derived iPSCs and showed that endothelial cells differentiated from the resulting inversion-corrected iPSCs expressed the *F8* gene in vitro and rescued the F8 deficiency in hemophilia A mice, demonstrating a proof of principle for iPSC-based treatment of hemophilia. To the best of our knowledge, this report is the first demonstration that chromosomal inversions or other large rearrangements can be corrected using RGENs or any other programmable nuclease in patient iPSCs. Chromosomal inversions are associated with other genetic diseases such as Hunter syndrome (Bondeson et al., 1995) and cancer (Nikiforova et al., 2000). Targeted genomic rearrangements using RGENs in iPSCs enable the creation of genome structural variations to study their functions and hold new promise in gene and cell therapy for the treatment of hemophilia A and other genetic diseases caused by large chromosomal rearrangements.

EXPERIMENTAL PROCEDURES

Design of RGENs

All guide RNAs (gRNAs) were designed using the online design tool available at http://www.rgenome.net.

Generation of iPSCs from Urine-Derived Cells

iPSCs were generated from urine-derived cells of severe hemophilia A patients by episomal reprogramming vectors or Sendai virus (Invitrogen).

Transfection of Cells

HeLa cells were transfected with Cas9- and gRNA-encoding plasmids using a Lipofectamine 2000 transfection reagent (Invitrogen). The iPSCs generated from urine-derived cells of hemophilia A patients were transfected with the same plasmids using a microporator system (Neon; Invitrogen) according to the manufacturer's protocol. For direct delivery of Cas9 protein and gRNA complex, purified recombinant Cas9 protein (Toolgen) was mixed with in vitro transcribed gRNA and electroporated.

Analysis of Genome Modifications

Activities of RGENs were determined by the T7E1 assay as described previously (Kim et al., 2009). The frequencies of targeted inversions at the F8 locus were estimated by digital PCR (Kim et al., 2010). Modified genome sequences of the targeted region in HeLa cells and iPSC cells were analyzed by Sanger sequencing.

Differentiation into Endothelial Cells and In Vivo Study

iPSCs were induced to differentiate into mature endothelial cells as described (Merkely et al., 2015). Hemophilia A mice (Jackson Laboratory, strain: B6; 129S4-*F8*^{tm1Kaz}/J) were used for the in vivo functional assay. Each mouse was injected with endothelial cells derived from iPSCs by subcutaneous injection into the hind-limb. Two weeks after transplantation, a tail-clip challenge was performed.

Tail-Clip Challenge and FVIII Activity Assay

The tail-clip assay was performed as described (Chao et al., 2001). In brief, the distal part of the tail, with a 1.5 mm diameter, was cut and allowed to bleed for 5 min. After firm pressure was applied to the tail for 1 min, the survival time was monitored. The Coamatic Factor VIII assay kit (Instrumentation Laboratory) was used to measure the FVIII activity according to the manufacturer's instructions. A standard curve was prepared by diluting the human calibration plasma (Instrumentation Laboratory).

Analysis of Off-Target Mutations Induced by RGENs

Unspecific cleavage by RGENs at potential off-target sites was analyzed by targeted deep sequencing and WGS of DNA from inversion-corrected iPSC clones. For targeted deep sequencing, potential off-target sites that differed from on-target sequences by up to four nucleotides were found with Cas-OFFinder (http://www.rgenome.net). Each PCR amplicon of a potential off-target site was subjected to paired-end read sequencing using MiSeq (Illumina). For WGS, genomic DNA from patient-derived iPSCs and inversion-corrected clones was fragmented and ligated with adapters to make libraries. Libraries were subjected to WGS using HiSeqXTen (Illumina) at Macrogen (South Korea) with a sequencing depth of 30.

For details on experimental procedures, see Supplemental Information.

SUPPLEMENTAL INFORMATION

Supplemental Information for this article includes three figures, three tables, and Supplemental Experimental Procedures and can be found with this article online at http://dx.doi.org/10.1016/j.stem.2015.07.001.

AUTHOR CONTRIBUTIONS

C.-Y.P., D.H.K., J.S.S., J.-H.K., D.-W.K., and J.-S.K. designed the study. C.-Y.P., D.H.K., J.S.S., J.J.S., J.L., and S.B. conducted the experiments and interpreted the results. C.-Y.P., D.H.K., J.S.S., J.-H.K., D.-W.K., and J.-S.K. wrote the manuscript. J.-H.K., D.-W.K., and J.-S.K. have contributed equally.

ACKNOWLEDGMENTS

D.-W.K. was supported by grants from the National Research Foundation of Korea (the Bio and Medical Technology Development Program, 2012M3A9B4028631 and 2012M3A9C7050126) and from the Korean Ministry of Health and Welfare (A120254). J.-S.K. was supported by a grant from IBS (IBS-R021-D1). J.-H.K. was supported by a grant from the National Research Foundation of Korea (2012M3A9C7050139). D.-W.K, J.-S.K, C.-Y.P, and D.H.K filed a patent application based on this work.

Received: December 5, 2014
Revised: May 14, 2015
Accepted: June 28, 2015
Published: July 23, 2015

REFERENCES

Bae, S., Park, J., and Kim, J.-S. (2014). Cas-OFFinder: a fast and versatile algorithm that searches for potential off-target sites of Cas9 RNA-guided endonucleases. Bioinformatics *30*, 1473–1475.

Bagnall, R.D., Giannelli, F., and Green, P.M. (2006). Int22h-related inversions causing hemophilia A: a novel insight into their origin and a new more discriminant PCR test for their detection. J. Thromb. Haemost. *4*, 591–598.

Bondeson, M.L., Dahl, N., Malmgren, H., Kleijer, W.J., Tönnesen, T., Carlberg, B.M., and Pettersson, U. (1995). Inversion of the IDS gene resulting from recombination with IDS-related sequences is a common cause of the Hunter syndrome. Hum. Mol. Genet. *4*, 615–621.

Chao, H., Monahan, P.E., Liu, Y., Samulski, R.J., and Walsh, C.E. (2001). Sustained and complete phenotype correction of hemophilia B mice following intramuscular injection of AAV1 serotype vectors. Mol. Ther. *4*, 217–222.

Cho, S.W., Kim, S., Kim, J.M., and Kim, J.S. (2013). Targeted genome engineering in human cells with the Cas9 RNA-guided endonuclease. Nat. Biotechnol. *31*, 230–232.

Cho, S.W., Kim, S., Kim, Y., Kweon, J., Kim, H.S., Bae, S., and Kim, J.S. (2014). Analysis of off-target effects of CRISPR/Cas-derived RNA-guided endonucleases and nickases. Genome Res. *24*, 132–141.

Cong, L., Ran, F.A., Cox, D., Lin, S., Barretto, R., Habib, N., Hsu, P.D., Wu, X., Jiang, W., Marraffini, L.A., and Zhang, F. (2013). Multiplex genome engineering using CRISPR/Cas systems. Science *339*, 819–823.

Cradick, T.J., Fine, E.J., Antico, C.J., and Bao, G. (2013). CRISPR/Cas9 systems targeting β-globin and CCR5 genes have substantial off-target activity. Nucleic Acids Res. *41*, 9584–9592.

Frock, R.L., Hu, J., Meyers, R.M., Ho, Y.J., Kii, E., and Alt, F.W. (2015). Genome-wide detection of DNA double-stranded breaks induced by engineered nucleases. Nat. Biotechnol. *33*, 179–186.

Fu, Y., Foden, J.A., Khayter, C., Maeder, M.L., Reyon, D., Joung, J.K., and Sander, J.D. (2013). High-frequency off-target mutagenesis induced by CRISPR-Cas nucleases in human cells. Nat. Biotechnol. *31*, 822–826.

Graw, J., Brackmann, H.H., Oldenburg, J., Schneppenheim, R., Spannagl, M., and Schwaab, R. (2005). Haemophilia A: from mutation analysis to new therapies. Nat. Rev. Genet. *6*, 488–501.

Hsu, P.D., Scott, D.A., Weinstein, J.A., Ran, F.A., Konermann, S., Agarwala, V., Li, Y., Fine, E.J., Wu, X., Shalem, O., et al. (2013). DNA targeting specificity of RNA-guided Cas9 nucleases. Nat. Biotechnol. *31*, 827–832.

Kim, H.J., Lee, H.J., Kim, H., Cho, S.W., and Kim, J.S. (2009). Targeted genome editing with zinc finger nucleases constructed via modular assembly. Genome Res. *19*, 1279–1288.

Kim, S., Lee, H.J., Kim, E., and Kim, J.S. (2010). Analysis of targeted chromosomal deletions induced by zinc finger nucleases. Cold Spring Harb. Protoc. http://dx.doi.org/10.1101/pdb.prot5477.

Kim, Y., Kweon, J., and Kim, J.S. (2013). TALENs and ZFNs are associated with different mutation signatures. Nat. Methods *10*, 185.

Kim, S., Kim, D., Cho, S.W., Kim, J., and Kim, J.S. (2014). Highly efficient RNA-guided genome editing in human cells via delivery of purified Cas9 ribonucleoproteins. Genome Res. *24*, 1012–1019.

Kim, D., Bae, S., Park, J., Kim, E., Kim, S., Yu, H.R., Hwang, J., Kim, J.I., and Kim, J.S. (2015). Digenome-seq: genome-wide profiling of CRISPR-Cas9 off-target effects in human cells. Nat. Methods *12*, 237–243, 1, 243.

Koo, T., Lee, J., and Kim, J.S. (2015). Measuring and reducing off-target activities of programmable nucleases including CRISPR-Cas9. Mol. Cells *38*, 475–481.

Lee, H.J., Kim, E., and Kim, J.S. (2010). Targeted chromosomal deletions in human cells using zinc finger nucleases. Genome Res. *20*, 81–89.

Lee, H.J., Kweon, J., Kim, E., Kim, S., and Kim, J.S. (2012). Targeted chromosomal duplications and inversions in the human genome using zinc finger nucleases. Genome Res. *22*, 539–548.

Mali, P., Yang, L., Esvelt, K.M., Aach, J., Guell, M., DiCarlo, J.E., Norville, J.E., and Church, G.M. (2013). RNA-guided human genome engineering via Cas9. Science *339*, 823–826.

Merkely, B., Gara, E., Lendvai, Z., Skopál, J., Leja, T., Zhou, W., Kosztin, A., Várady, G., Mioulane, M., Bagyura, Z., et al. (2015). Signaling via PI3K/FOXO1A pathway modulates formation and survival of human embryonic stem cell-derived endothelial cells. Stem Cells Dev. *24*, 869–878.

Nikiforova, M.N., Stringer, J.R., Blough, R., Medvedovic, M., Fagin, J.A., and Nikiforov, Y.E. (2000). Proximity of chromosomal loci that participate in radiation-induced rearrangements in human cells. Science *290*, 138–141.

Pandey, G.S., Yanover, C., Miller-Jenkins, L.M., Garfield, S., Cole, S.A., Curran, J.E., Moses, E.K., Rydz, N., Simhadri, V., Kimchi-Sarfaty, C., et al.; PATH (Personalized Alternative Therapies for Hemophilia) Study Investigators (2013). Endogenous factor VIII synthesis from the intron 22-inverted F8 locus may modulate the immunogenicity of replacement therapy for hemophilia A. Nat. Med. *19*, 1318–1324.

Park, C.Y., Kim, J., Kweon, J., Son, J.S., Lee, J.S., Yoo, J.E., Cho, S.R., Kim, J.H., Kim, J.S., and Kim, D.W. (2014). Targeted inversion and reversion of the blood coagulation factor 8 gene in human iPS cells using TALENs. Proc. Natl. Acad. Sci. USA *111*, 9253–9258.

Pattanayak, V., Lin, S., Guilinger, J.P., Ma, E., Doudna, J.A., and Liu, D.R. (2013). High-throughput profiling of off-target DNA cleavage reveals RNA-programmed Cas9 nuclease specificity. Nat. Biotechnol. *31*, 839–843.

Ran, F.A., Cong, L., Yan, W.X., Scott, D.A., Gootenberg, J.S., Kriz, A.J., Zetsche, B., Shalem, O., Wu, X., Makarova, K.S., et al. (2015). In vivo genome editing using Staphylococcus aureus Cas9. Nature *520*, 186–191.

Shahani, T., Lavend'homme, R., Luttun, A., Saint-Remy, J.M., Peerlinck, K., and Jacquemin, M. (2010). Activation of human endothelial cells from specific vascular beds induces the release of a FVIII storage pool. Blood *115*, 4902–4909.

Smith, C., Gore, A., Yan, W., Abalde-Atristain, L., Li, Z., He, C., Wang, Y., Brodsky, R.A., Zhang, K., Cheng, L., and Ye, Z. (2014). Whole-genome sequencing analysis reveals high specificity of CRISPR/Cas9 and TALEN-based genome editing in human iPSCs. Cell Stem Cell *15*, 12–13.

Suzuki, K., Yu, C., Qu, J., Li, M., Yao, X., Yuan, T., Goebl, A., Tang, S., Ren, R., Aizawa, E., et al. (2014). Targeted gene correction minimally impacts whole-genome mutational load in human-disease-specific induced pluripotent stem cell clones. Cell Stem Cell *15*, 31–36.

Tsai, S.Q., Zheng, Z., Nguyen, N.T., Liebers, M., Topkar, V.V., Thapar, V., Wyvekens, N., Khayter, C., Iafrate, A.J., Le, L.P., et al. (2015). GUIDE-seq enables genome-wide profiling of off-target cleavage by CRISPR-Cas nucleases. Nat. Biotechnol. *33*, 187–197.

Veres, A., Gosis, B.S., Ding, Q., Collins, R., Ragavendran, A., Brand, H., Erdin, S., Cowan, C.A., Talkowski, M.E., and Musunuru, K. (2014). Low incidence of off-target mutations in individual CRISPR-Cas9 and TALEN targeted human stem cell clones detected by whole-genome sequencing. Cell Stem Cell *15*, 27–30.

Wang, X., Wang, Y., Wu, X., Wang, J., Wang, Y., Qiu, Z., Chang, T., Huang, H., Lin, R.J., and Yee, J.K. (2015). Unbiased detection of off-target cleavage by CRISPR-Cas9 and TALENs using integrase-defective lentiviral vectors. Nat. Biotechnol. *33*, 175–178.